



Christiansen, E., Hudson, B. D., Hansen, A. H., Milligan, G., and Ulven, T. (2016) Development and characterization of a potent free fatty acid receptor 1 (FFA1) fluorescent tracer. *Journal of Medicinal Chemistry*, 59(10), pp. 4849-4858. (doi:[10.1021/acs.jmedchem.6b00202](https://doi.org/10.1021/acs.jmedchem.6b00202))

This is the author's final accepted version.

There may be differences between this version and the published version. You are advised to consult the publisher's version if you wish to cite from it.

<http://eprints.gla.ac.uk/118427/>

Deposited on: 14 April 2016

Enlighten – Research publications by members of the University of Glasgow  
<http://eprints.gla.ac.uk>

# Development and characterization of a potent free fatty acid receptor 1 (FFA1) fluorescent tracer

*Elisabeth Christiansen<sup>†1</sup>, Brian D. Hudson<sup>‡1</sup>, Anders Højgaard Hansen<sup>†</sup>, Graeme Milligan<sup>‡</sup> and Trond Ulven<sup>†,\*</sup>*

<sup>1</sup>These authors have contributed equally.

<sup>†</sup>Department of Physics, Chemistry and Pharmacy, University of Southern Denmark, Campusvej 55, DK-5230 Odense M, Denmark

<sup>‡</sup>Molecular Pharmacology Group, Institute of Molecular, Cell and Systems Biology, College of Medical, Veterinary and Life Sciences, University of Glasgow, Glasgow G12 8QQ, Scotland, United Kingdom

## ABSTRACT

The free fatty acid receptor 1 (FFA1/GPR40) is a potential target for treatment of type 2 diabetes. Although several potent agonists have been described, there remains a strong need for suitable tracers to interrogate ligand binding to this receptor. We address this by exploring fluorophore-tethering to known potent FFA1 agonists. This led to the development of **4**, a high affinity FFA1 tracer with favorable and polarity-dependent fluorescent properties. A close to ideal overlap between the emission spectrum of the NanoLuciferase receptor tag and the excitation spectrum of **4** enabled the establishment of a homogenous BRET-based binding assay suitable for both detailed kinetic studies and high throughput competition binding studies. Using **4** as a tracer demonstrated that the compound acts fully competitively with selected synthetic agonists but not with lauric acid and allowed for the characterization of binding affinities of a diverse selection of known FFA1 agonists, indicating that **4** will be a valuable tool for future studies at FFA1.

## INTRODUCTION

Free fatty acid receptor 1 (FFA1, also known as GPR40) is a 7TM receptor activated by medium- and long-chain free fatty acids that in recent years has attracted much attention as a potential target for the treatment of type 2 diabetes. FFA1 is highly expressed in pancreatic  $\beta$ -cells where it enhances insulin secretion in a glucose concentration-dependent manner. It may therefore represent a target for safe new insulin secretagogues devoid of the risk of hypoglycemia associated with the currently used sulfonylureas.<sup>1</sup> FFA1 is also highly expressed in enteroendocrine cells and regulates incretin hormone secretion, driving further interest in this receptor as a target for type 2 diabetes.<sup>2</sup> Proof of this concept was recently provided from clinical trials with **1** (TAK-875/fasiglifam), a selective FFA1 agonist that showed glucose lowering activity similar to the sulfonylurea glimepiride without the increased hypoglycemic events observed with glimepiride.<sup>3</sup> Originally derived from the structure of docosahexaenoic acid (DHA),<sup>4</sup> the pharmacology of **1** has turned out to be more complex than previously presumed. Rather than binding to the orthosteric free fatty acid binding site on FFA1, **1** was recently shown to be an allosteric agonist with the ability to positively modulate fatty acid actions at FFA1.<sup>5</sup> In fact, studies using radiolabeled ligands have indicated that FFA1 possesses at least three distinct binding sites that recognize structurally closely related ligands and that each site is able to allosterically modulate ligand function at the others.<sup>6</sup> The recently published crystal structure of FFA1 in complex with **1** lent further support to the concept of multiple FFA1 binding sites, revealing several potential binding sites in addition to the site of **1**.<sup>7</sup> Most importantly from a drug development standpoint, the specific binding site an FFA1 agonist interacts with may influence the ligand's downstream signaling outcomes,<sup>2c</sup> and thus may have clear implications for the ultimate therapeutic efficacy of any developed FFA1 agonists. How these structurally

similar ligands interact with their distinct binding sites on FFA1 remains poorly understood and, therefore, there is a clear need to develop novel tools to assess ligand binding to this receptor.

Ligands incorporating fluorescent probes have become common tools to assess ligand binding to GPCRs and offer a number of advantages over classic radiolabeled ligands.<sup>8</sup> In addition to practical considerations of convenience, safety and cost, by utilizing solvatochromic fluorophores or combining with a resonance energy transfer assay format, fluorescent ligands provide the significant advantage of real-time detection of their binding. This allows for homogenous assay formats, improved measurements of ligand binding kinetics, and visualizations of receptor-ligand complexes within a living cell.<sup>8-9</sup> Fluorescently-tagged FFA1 ligands are, therefore, expected to be valuable tools for elucidation of the pharmacology of this very interesting antidiabetic target.

### **Choice of fluorophore**

Commonly used fluorophores include relatively large structures such as fluorescein derivatives and especially BODIPY (4,4-difluoro-4-bora-3a,4a-diaza-*s*-indacene) due to its several favorable properties.<sup>10</sup> The smaller benzofurazan core structure is also well-known in fluorogenic and fluorescent reagents and represents a class of compounds that results in derivatives with good quantum yields and with excitation and emission wavelengths long enough to avoid interference from biological autofluorescence.<sup>11</sup> Variation of substituents in the 4- and 7-position influences the electronic effects on the system and thereby the fluorescent properties.<sup>12</sup> In this way the excitation and emission maxima as well as fluorescent intensity can be modified. The 4-nitro-7-aminobenzofurazan (NBD) fluorophore is a relatively small fluorescent probe with excitation maximum around 470 nm and emission maximum around 530 nm when substituted with an amine in the 7-position,<sup>13</sup> wavelengths well suited to *in vitro* biological systems. Furthermore,

NBD is solvatochromic, exhibiting very low fluorescent activity in polar and protic environments, but much increased fluorescence in hydrophobic environments such as protein binding pockets or the plasma membrane.<sup>14</sup> These properties suggest an NBD fluorescent tracer may possess reduced background fluorescence from non-bound fluorescent tracer allowing for both homogenous detection and use in imaging applications. NBD has been used previously for labeling small amine containing molecules and proteins used in binding assays as well as for visualization in living cells.<sup>15</sup>

### Design of fluorescent FFA1-tracers

We have previously reported on two series of agonists for FFA1 based on an alkyne scaffold and a benzyloxy/benzylamine scaffold, respectively, and we aimed at exploring both series in efforts to develop a potent fluorescent tool compound for FFA1 (Figure 1).

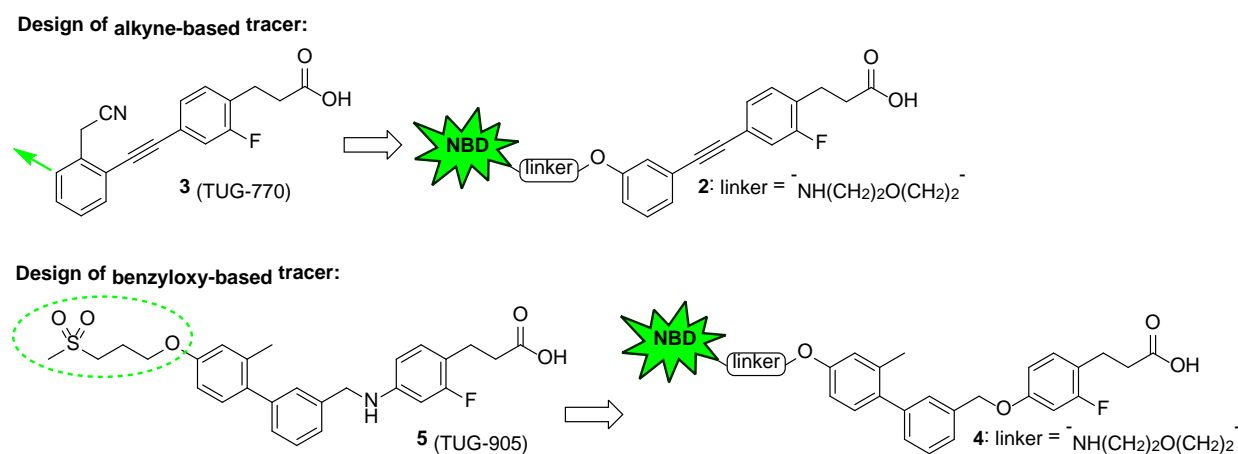


**Figure 1.** Design strategies of alkyne-based and benzyloxy-based fluorescent tracers. NBD, 7-nitrobenzofurazan-4-yl.

The first fluorescent tracer **2** is based on the alkyne series that includes **3** (TUG-770), a compound showing good potency and lower lipophilicity than most other FFA1 agonists.<sup>16</sup> This is important because incorporation of a fluorophore generally erodes potency and, for uncharged

fluorophores, increases lipophilicity of the compounds thereby reducing their usefulness for *in vitro* pharmacology studies. Structure-activity relationship (SAR) investigations have shown that larger substituents at the alkyne scaffold are best tolerated in the *meta*-position of the terminal phenyl ring, but these lead to a loss in potency, which to some extent can be regained by introduction of a 2-fluoro substituent on the central phenyl ring.<sup>16-17</sup> Thus, the 2-fluoro substituent was incorporated in the target structure and the spacer-extended fluorophore was attached to the *meta*-position of the terminal phenyl ring. A shorter 2-aminoethoxy and a longer 2-(2-aminoethoxy)ethoxy tether were considered, however, the NBD-tethered compounds with the shorter 2-aminoethoxy spacer turned out to be unstable and decomposed before or during purification. Focus was therefore directed towards the longer linker.

The second fluorescent tracer **4** was designed based on the benzylamine agonist **5** (TUG-905), a potent and selective agonist on both the human and rodent FFA1 receptors.<sup>18</sup> The 2-fluoro substituent, shown to significantly enhance potency in the alkyne series,<sup>16</sup> also in some cases enhances potency in the benzylamine and benzyloxy series and was incorporated in the target structure. The amine-linker was exchanged for the corresponding oxy-linker since this facilitates preparation and the modification has been shown to have only modest effect on ligand potency.<sup>19</sup> The mesylpropoxy appendage also present in the structurally related agonist **1**, has been found to reduce lipophilicity of the compounds with little or no effect on potency.<sup>4b, 18</sup> The crystal structure of FFA1 in complex with **1** provided an explanation for this in showing the mesylpropoxy appendage to be protruding from the ligand binding pocket towards the lipid bilayer.<sup>7</sup> Thus, this seems to be an optimal linkage point for attachment of a spacer-extended fluorophore. In order to gain optimal fluorescent properties of the NBD fluorophore the compound should be attached to a primary aliphatic amine.<sup>12</sup> Thus, we decided to explore 2-(2-

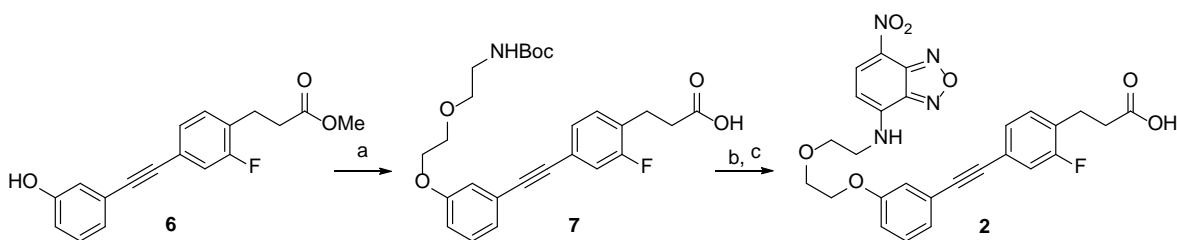
aminoethoxy)ethanol, which is slightly longer than the mesylpropoxy substituent but less lipophilic than an all carbon linker.

## RESULTS AND DISCUSSION

### Synthesis of tracer ligands

The fluorescent tracer molecules **2** and **4** were synthesized by similar strategies. Tracer **2** was synthesized from the previously published alkyne intermediate **6**<sup>16</sup> by alkylation with Boc-protected 2-(2-aminoethoxy)ethyl tosylate to give **7**,<sup>20</sup> followed by concomitant acid catalyzed ester hydrolysis and Boc-deprotection to give the zwitterionic intermediate that was used directly in the reaction with NBD chloride and purification by preparative HPLC gave **2** in 24% yield from **6**.

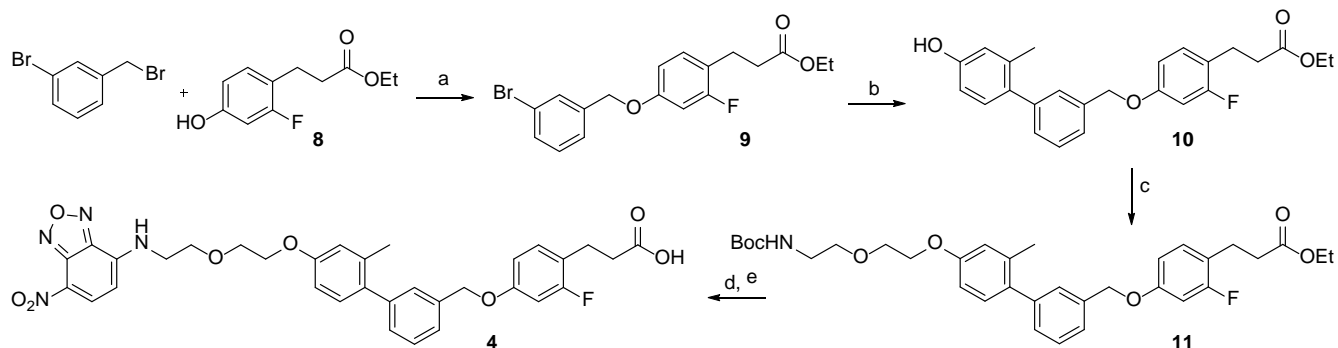
#### Scheme 1. Synthesis of **2**.<sup>a</sup>



<sup>a</sup> Reagents and conditions: (a) BocNH(CH<sub>2</sub>)<sub>2</sub>O(CH<sub>2</sub>)<sub>2</sub>OTs, K<sub>2</sub>CO<sub>3</sub>, MeCN, reflux, 3 h, 79%. (b) HCl<sub>(aq)</sub>, THF, reflux, 2½ h, 57%. (c) NBDCl, NaHCO<sub>3</sub>, MeOH, 50 °C, 4 h, 54%.

Tracer molecule **4** was synthesized from **8**, first by a Williamson ether synthesis to provide **9** and further by a two-step one-pot borylation Suzuki cross-coupling using tetrahydroxydiboron as borylation agent and the second generation XPhos precatalyst to give **10** (Scheme 2).<sup>21</sup> The fluorophore was installed by alkylation of the phenol of **10**, deprotection of **11** and reaction with NBD chloride, as described for **2**, to provide **4** in 8% overall yield from **8**.

## Scheme 2. Synthesis of **4**.<sup>a</sup>



<sup>a</sup>Reagents and conditions: (a) K<sub>2</sub>CO<sub>3</sub>, acetone, rt, 16 h, 81%. (b) BBA, XPhos, Pd-G2-XPhos, KOAc, EtOH, 80 °C, 2 h, then 4-bromo-3-methylphenol, 1.8 M K<sub>2</sub>CO<sub>3(aq)</sub>, 80 °C, 16 h, 37%. (c) BocNH(CH<sub>2</sub>)<sub>2</sub>O(CH<sub>2</sub>)<sub>2</sub>OTs, K<sub>2</sub>CO<sub>3</sub>, MeCN, reflux, 23 h, 93%. (d) HCl<sub>(aq)</sub>, THF, reflux 7 h. (e) NBDCl, NaHCO<sub>3</sub>, MeOH, 50 °C, 4 h, 28%.

### Characterization of fluorescent properties

The fluorescent properties of the ligands were examined in Hanks' balanced salt solution (HBSS) supplemented with calcium and magnesium, a standard aqueous buffer used for our *in vitro* pharmacological assays, and *n*-octanol mimicking a lipophilic environment to examine the solvatochromic effect of NBD.

The excitation and emission maxima of **2** in *n*-octanol were within the desired range giving an acceptable Stokes shift (SS) of 64 nm (Table 1). As expected, the excitation and emission maxima were somewhat red-shifted in the aqueous medium ( $\lambda_{\text{ex}} = 483 \text{ nm}$  &  $\lambda_{\text{em}} = 546 \text{ nm}$ , Table 1 and Figure S1). Compound **4** showed excitation and emission maxima similar to **2** in both *n*-octanol and HBSS (SS = 65 nm, Figure 2A), however, the extinction coefficient was 2.7-fold higher for **4**. To investigate the influence of the solvatochromic effect of NBD, emission spectra of **4** were recorded in both *n*-octanol and HBSS using identical instrument settings. This showed, as expected, almost no fluorescent activity in the aqueous environment (Figure 2B), too low to determine the quantum yield. Background fluorescence from unbound excess tracer in

aqueous media should therefore not be an issue. Overall, both tracers demonstrated good fluorescent properties with **2** showing a somewhat higher quantum yield (Table 1). The initial biological characterization of these ligands at FFA1, however, found **4** to be superior with both  $EC_{50}$  and  $K_d$ -value in the nanomolar range.

**Table 1.** Basic *in vitro* and fluorescent characterization of tracers.

	$Ca^{2+}$ assay	Binding Assay			<i>n</i> -Octanol		HBSS		
	$EC_{50}^a$ [nM]	$K_d^b$ [nM]	$\gg_{ex}$ [nm]	$\gg_{em}$ [nm]	SS [nm]	$\mu$ [ $M^{-1}cm^{-1}$ ]	QY	$\gg_{ex}$ [nm]	$\gg_{em}$ [nm]
<b>2</b>	>1,000 <sup>c</sup>	n.d. <sup>d</sup>	462	526	64	$7969 \pm 126$	0.65	483	546
<b>4</b>	187	$7.4 \pm 1.3$	462	527	65	$21820 \pm 37$	0.44	478	545

<sup>a</sup>Potency of  $Ca^{2+}$  response in Flp-In T-REx 293 cells induced to express FFA1. <sup>b</sup> $K_d$  was determined from saturation BRET binding assay using **5** to define non-specific binding. <sup>c</sup>**2** generated an FFA1-dependent  $Ca^{2+}$  response, however its potency was too low to fit a concentration-response and establish an  $EC_{50}$  value. <sup>d</sup>Not determined. SS, Stokes shift; QY, quantum yield.

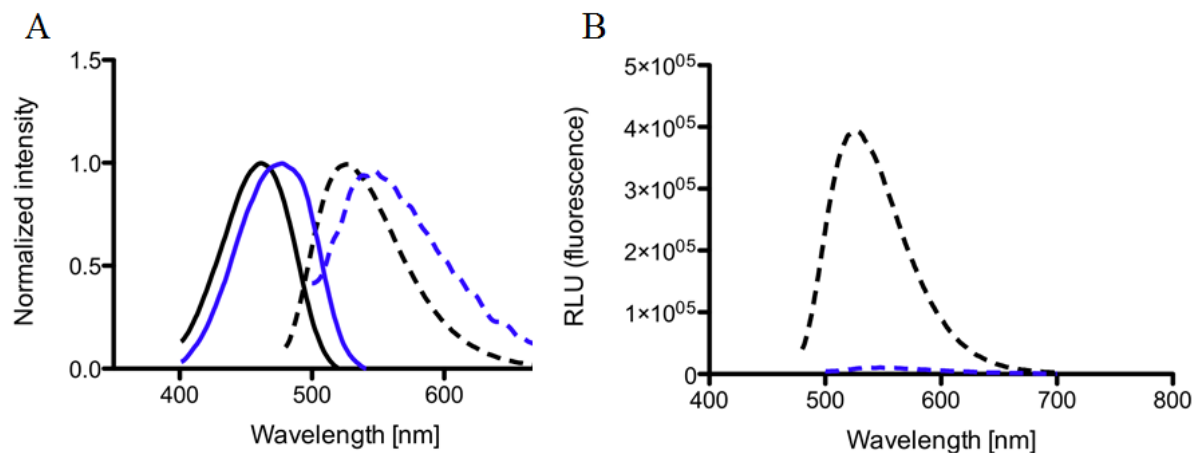


**Figure 2.** Fluorescent properties of **4**. A) Excitation & emission spectra. B) Solvent effect on emission spectra; -- *n*-octanol, -- HBSS, solid line ~ excitation, dotted line ~ emission. RLU, relative luminescence units.

## Functional characterization of 2 and 4

Initial functional characterization of **2** established that although the fluorophore remained an FFA1 agonist, it had substantially reduced potency compared to the parent compound **3**. Indeed, its potency was too low to establish an accurate  $EC_{50}$  value (Table 1, Figure 3A). In contrast, while **4** also behaved as an agonist, this compound retained high potency, displaying only a small reduction compared to its parent **5** (Table 1, Figure 3B). This suggests the position of the linker and the NBD fluorophore in **4** has minimal impact on its interaction with FFA1, and that the molecule is likely to be a useful FFA1 tracer.

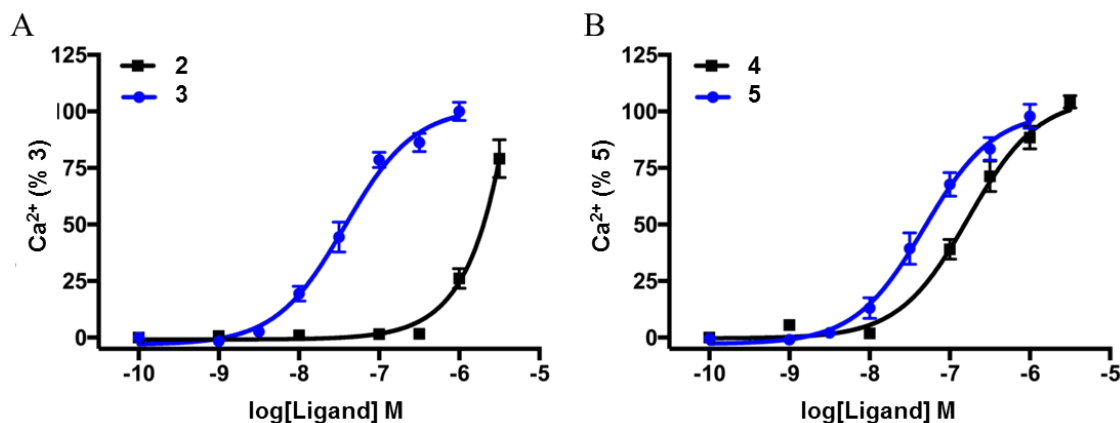
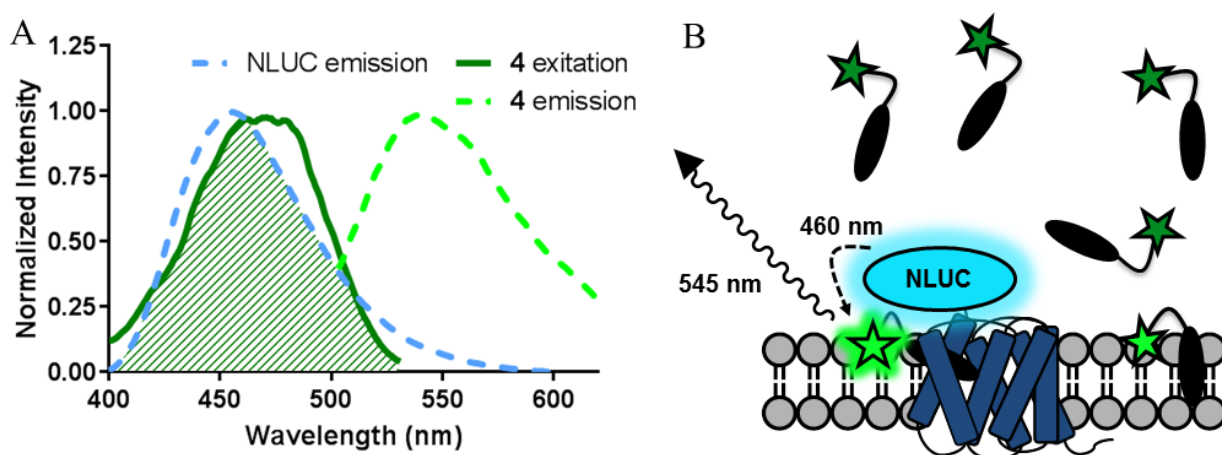


**Figure 3.** High potency at FFA1 is maintained for the NBD labeled **4**. A) Concentration-response curves generated using Flp-In T-REx 293 FFA1-eYFP cells are shown for **2** and its parent compound **3**. B) Concentration-response curves in these cells are shown for **4** and its parent compound **5**. Data shown as mean  $\pm$  S.E.M., n=3.

## Characterization of 4 as an FFA1 tracer

Based on its high potency in the  $Ca^{2+}$  assay we developed an FFA1 binding assay utilizing this ligand as a tracer employing a bioluminescence resonance energy transfer (BRET)-based approach.<sup>22</sup> This allows for a truly homogeneous ‘mix and measure’ assay, well suited for both detailed kinetic as well as high throughput equilibrium binding experiments. For this, FFA1 was

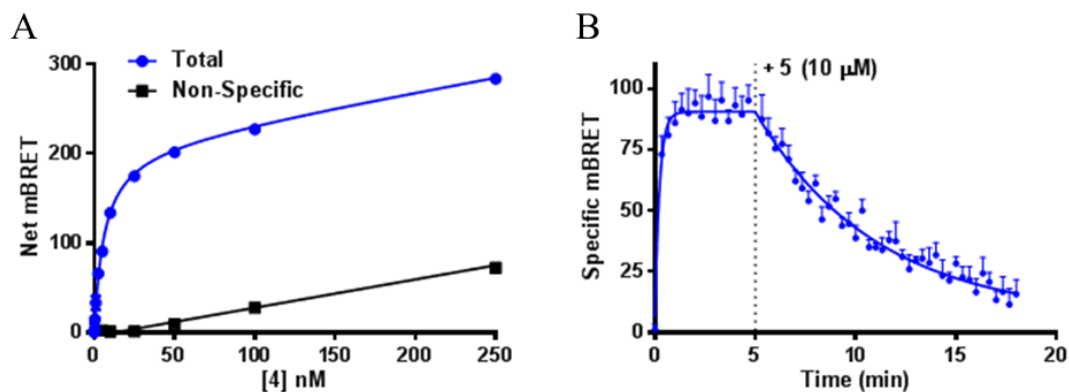
tagged at its N-terminus with the small, bright NanoLuciferase (NLUC), a bioluminescent enzyme with an emission spectrum that has excellent overlap with the NBD excitation spectrum (Figure 5A). Thus, when **4** binds to NLUC-FFA1, energy transfer at 460 nm can occur between the NLUC and NBD moiety, resulting in NBD emission at 545 nm. As BRET is strictly dependent on the distance between the bioluminescent and fluorescent partners, this approach eliminates the need to remove **4** from the assay medium and limits any signal obtained from the non-specific binding of **4** to the membrane (Figure 5B).



**Figure 5.** Compound **4** is suitable for use in a BRET-based binding assay. A) The emission spectrum of NLUC (blue stippled) along with the excitation (dark green) and emission (light green stippled) spectra of **4**, as measured under binding assay conditions, are shown. The spectral overlap between NLUC emission and **4** excitation is marked by the diagonal green fill. B) A cartoon depicting the concept of the BRET binding assay is shown. Light is emitted from receptor bound NLUC at 460 nm and, through BRET, transferred only to the fluorophore in very close proximity. This in turn results in emission at 545 nm by the receptor bound fluorophore, but not by the unbound fluorophore in the medium, nor by the non-specifically bound fluorophore in the membrane. The solvatochromic properties of NBD should further reduce any

signal from unbound **4**, due to reduced fluorescence from the molecules in the aqueous buffer environment vs those in the membrane (shown by different shade of green).

Saturation BRET binding experiments with **4** showed low non-specific BRET at concentrations up to 100 nM (Figure 6A), a highly satisfactory result considering the lipophilicity of the compound ( $\text{clogP} = 7.77$ ). This low ratio of total to non-specific signal allowed determination of the dissociation constant for **4** through equilibrium saturation binding experiments (Table 1, Figure 6A). Kinetic binding experiments were also conducted, establishing the off- and on-rates for **4** to be:  $k_{\text{off}} = 0.166 \pm 0.017 \text{ min}^{-1}$  and  $k_{\text{on}} = 41,100,000 \pm 7,800,000 \text{ min}^{-1} \text{ M}^{-1}$  (Figure 6B). Independent derivation of the  $K_d$  for **4** from the  $k_{\text{on}}$  and  $k_{\text{off}}$  values yielded a  $K_d$  value of 4.0 nM, in close accord with the  $K_d$  value obtained from saturation binding experiments (Table 1).

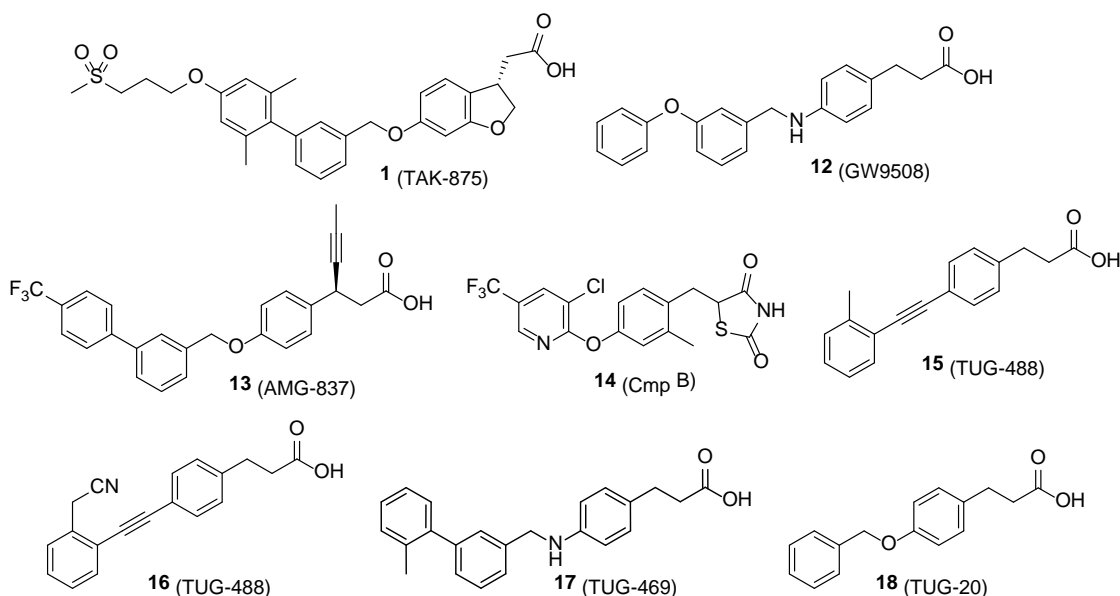


**Figure 6.** Saturation and kinetic binding experiments allow determination of the affinity of **4** at FFA1. A) A representative saturation binding experiment is shown, where non-specific binding is defined by co-incubation with 10  $\mu\text{M}$  **5**. Data shown are mean  $\pm$  S.E.M. of technical triplicates. B) A representative kinetic binding experiment is shown. Association was initiated by the addition of **4** (100 nM) followed by the addition of 10  $\mu\text{M}$  **5** at 5 min to prevent re-binding of

**4** subsequent to dissociation of the fluorescent tracer. Data shown are mean  $\pm$  S.E.M. of technical triplicates.

Next, **4** was used as a tracer in competition binding assays to assess the affinity of previously published FFA1 agonists. Given the previous reports demonstrating multiple FFA1 binding sites,<sup>6-7</sup> it was first important to determine which classes of FFA1 agonist do, and do not, bind competitively with **4**. For this, competition binding experiments were conducted using the synthetic agonists **1**, **3**, **5**, and **12** (GW9508),<sup>23</sup> as well as with the endogenous agonist lauric acid, against varying concentrations of **4** (Figure S2). From these experiments, it was clear that each synthetic agonist fully competed with **4**, even when the concentration of **4** was greater than 20 times  $K_d$ . This strongly suggests that each of these compounds binds competitively with **4** to FFA1. By contrast, despite acting as an FFA1 agonist, lauric acid only resulted in a minor reduction of the specific binding signal of **4**, suggesting that it does not bind competitively. This finding is consistent with previous reports that the fatty acids bind to a different site than many synthetic FFA1 agonists.<sup>5-6</sup> Global curve fitting to an allosteric ternary complex model of the lauric acid data allowed for an estimation of its  $pK_B$  ( $4.46 \pm 0.15$ ) and allosteric cooperativity factor ( $\log\alpha = -0.29 \pm 0.09$ ) values.

Given that we observed all synthetic agonist classes to be competitive with **4**, we next aimed to use this compound to assess the affinity of a range of previously reported FFA1 agonists. For these studies, in addition to parent compounds and analogues of **2** and **4**, the first high-potency FFA1 agonist **12**, the previous clinical candidates **13** (AMG-837)<sup>24</sup> and **1**, and Merck's potent thiazolidinedione agonist **14** (Cmp B)<sup>25</sup> were selected.<sup>23-26</sup> Each of the selected molecules exhibited competitive binding with **4** that allowed estimation of  $K_i$  binding affinity constants (Table 2).

**Table 2.** Potency and binding affinity of selected FFA1 agonists.

	Competition binding $pK_i^a$	$\beta$ -Arrestin <sup>b</sup> $pEC_{50}$ (% $E_{max}$ )	Calcium <sup>c</sup> $pEC_{50}$ (% $E_{max}$ )
<b>1</b>	$7.54 \pm 0.03$	$8.03 \pm 0.13$ (89)	$7.24 \pm 0.01$ (108)
<b>3</b>	$7.07 \pm 0.04$	$7.73 \pm 0.06$ (100)	$8.23 \pm 0.06$ (100)
<b>5</b>	$8.36 \pm 0.01$	$7.85 \pm 0.02$ (106)	$8.04 \pm 0.02$ (102) <sup>d</sup>
<b>12</b>	$6.66 \pm 0.05$	$7.55 \pm 0.15$ (86)	$7.54 \pm 0.03$ (103) <sup>d</sup>
<b>13</b>	$7.38 \pm 0.06$	$6.81 \pm 0.50$ (108)	$6.77 \pm 0.06$ (105)
<b>14</b>	$7.16 \pm 0.03$	$7.26 \pm 0.03$ (95)	$6.75 \pm 0.04$ (103) <sup>d</sup>
<b>15</b>	$6.20 \pm 0.05$	$7.17 \pm 0.07$ (100)	$7.34 \pm 0.07$ (103) <sup>d</sup>
<b>16</b>	$6.69 \pm 0.04$	$7.21 \pm 0.10$ (95)	$7.70 \pm 0.04$ (103) <sup>d</sup>
<b>17</b>	$8.23 \pm 0.03$	$7.95 \pm 0.03$ (114)	$7.73 \pm 0.04$ (114) <sup>d</sup>
<b>18</b>	$4.86 \pm 0.02$	$6.26 \pm 0.09$ (90)	$6.34 \pm 0.02$ (100) <sup>d</sup>
Lauric acid	– <sup>e</sup>	$5.10 \pm 0.06$ (130)	$6.12 \pm 0.05$ (116)

<sup>a</sup> $pK_i$  values obtained through displacement BRET binding assays containing 10 nM **4**,  $n = 3$ .  
<sup>b</sup> $\beta$ -arrestin  $pEC_{50}$  determined using BRET- $\beta$ -arrestin recruitment assay.  $E_{max}$  expressed as % of **3**,  $n = 3$ .  
<sup>c</sup> $Ca^{2+}$   $pEC_{50}$  were determined using FFA1-expressing 132N1 cells.  $E_{max}$  is expressed as % of **3**,  $n = 3$ .  
<sup>d</sup>Previously published.<sup>16-19</sup> <sup>e</sup>Partial competition that fitted to an allosteric ternary complex model gave  $pK_B = 4.46$  and  $\log\alpha = -0.29$  (see Figure S2).

Overall, good correlation between agonist potency and binding  $K_i$ -values was observed, with **5** being both the most potent agonist in the functional assays and the ligand with the highest affinity (Table 2). Likewise, **1** and **13** showed  $K_i$ -values that were similar to their functional potency, and also similar to  $K_i$ -values previously established through a radiotracer competition binding assay.<sup>2c</sup> **14**, which with a different core structure and a thiazolidinedione head group is the most structurally distinct from **4**, also exhibited potency in the functional assays that corresponded well to its binding affinity. In contrast, **3**, a highly potent agonist in both  $\text{Ca}^{2+}$  and  $\beta$ -arrestin-2 interaction-based functional assays, showed a 15- and 3-fold lower potency, respectively, in the binding assay. A similar observation was made with **12**, also showing a much lower affinity for FFA1 than would be expected based on the functional data.

To examine the discrepancy between potency and affinity of **3** more closely, derivatives of **3** and **5** with varying functional potency were tested in competition binding assays. These studies included **3**, **15** (TUG-424)<sup>27</sup> and **16** (TUG-488)<sup>17</sup> in the alkyne series and showed correct ranking within the series, i.e. **3** > **16** > **15**, and excellent correlation between binding affinity and calcium mobilization ( $R^2 = 0.967$ ). Likewise, the functional SAR within the benzylamine/oxy dihydrocinnamic acid series including **5**, **12**, **17** (TUG-469)<sup>19</sup> and **18** (TUG-20)<sup>19</sup> shows correct ranking (**5** > **17** > **12** >> **18**) and good correlation between binding affinity and calcium mobilization ( $R^2 = 0.913$ ), whereas the  $\beta$ -substituted **13** and **1** were fitted well with the other benzylamine/oxy compounds ( $R^2 = 0.709$ ). The overall correlation is, however, relatively low ( $R^2 = 0.345$ ). Together this demonstrates that although the affinity obtained through competition with **4** generally correlates well with functional potency within a specific FFA1 agonist series,

the relationship between affinity and functional potency may vary between structurally distinct compounds.

The discrepancy between affinity and potency across chemical series may be explained by differences in the intrinsic efficacy of these series to activate FFA1. Although all agonists tested appeared to be equal and full agonists in the  $\text{Ca}^{2+}$  assay, it is well established that in  $\text{Ca}^{2+}$  assays, which have a high level of signal amplification, differences in intrinsic efficacy of a ligand will often manifest as increased potency, due to the presence of a receptor reserve.<sup>28</sup> It could also be related to kinetic properties where slow and fast ligands may have distinct functional activities but will appear to have the same affinity as long as the ratios between their on- and off-rates are the same. It is therefore possible that at least some aspects of the discrepancy between potency and affinity observed for certain chemical series of FFA1 agonists could be related to binding kinetics. A third factor that may contribute to the discrepancy is the apparent presence of the multiple binding sites in FFA1,<sup>5-6</sup> implying the possibility of partial or lack of overlap with **4**. In line with these observations, lauric acid was found to behave as an allosteric compound incompetent to fully displace **4**, in contrast to the synthetic agonists that all behaved as fully competitive with **4**, indicating at least partially overlapping binding sites. Taken together, these findings demonstrate that a full characterization of both binding affinity and functional potency will be critical to understanding the pharmacology of novel FFA1 compounds.

## **CONCLUSION**

Taking advantage of established SAR of known agonists, we have developed fluorescent FFA1 tracers by tethering of the NBD fluorophore to potent core structures. This resulted in the identification of **4**, a high affinity fluorescent tracer molecule with a favorable specific to non-specific binding signal at up to 100 nM concentration. The compound possesses good

spectroscopic properties with close to absent fluorescence in aqueous environments but a high quantum yield, extinction coefficient and Stokes shift in non-polar environments. We have demonstrated the efficient use of **4** in a homogenous ‘mix and measure’ BRET-based binding assay suitable for both detailed kinetic studies and high throughput competition binding studies. This establishes **4** as a valuable tool in future drug discovery efforts targeting FFA1.

## **EXPERIMENTAL SECTION**

### **Synthesis**

Commercial starting materials and solvents were used without further purification, unless otherwise stated. THF was freshly distilled from sodium/benzophenone. MeOH and MeCN were dried over 3 Å sieves. K<sub>2</sub>CO<sub>3</sub> was dried and stored in an oven. TLC was performed on TLC silica gel 60 F254 plates and visualized at 254 or 365 nm or by staining with phosphomolybdic acid, ninhydrin, FeCl<sub>3</sub> or KMnO<sub>4</sub> stains. Purification by flash chromatography was carried out using silica gel 60 (0.040-0.063 mm, Merck). <sup>1</sup>H, <sup>13</sup>C and <sup>19</sup>F NMR spectra were recorded at 400, 101, and 376 MHz, respectively, on Bruker Avance III 400 at 300 K. HPLC analysis was performed using a Gemini C18 column (5 μm, 4.6x150 mm); flow: 1 mL/min; 10% MeCN in water (0-1 min), 10-100% MeCN in water (1-10 min), 100% MeCN (11-15 min), with both solvents containing 0.1% HCOOH as modifier; UV detection at 254 nm. HPLC purification was performed by using a Phenomenex Luna C18 column (5 μm, 250x21.20 mm) with gradient elution of MeCN and H<sub>2</sub>O, with both solvents containing 0.1% HCOOH as modifier. High-resolution mass spectra (HRMS) were obtained on a Bruker micrOTOF-Q II (ESI). Purity was determined by HPLC and confirmed by inspection of NMR spectra. The purity of all test compounds were >95%.

**3-(2-Fluoro-4-((3-(2-(2-((7-nitrobenzo[c][1,2,5]oxadiazol-4-yl)amino)ethoxy)ethoxy)-phenyl)ethynyl)phenyl)propanoic acid (2).** *Step 1:* **7** (176 mg, 0.36 mmol) was dissolved in THF (4 mL). 4M HCl<sub>(aq)</sub> (2 mL) was added and the reaction was heated to reflux for 2½ h. After complete hydrolysis the reaction was cooled to room temperature and 2M NaOH<sub>(aq)</sub> (4 mL) was added. The mixture was extracted with EtOAc (x3). Additional 2M NaOH<sub>(aq)</sub> (2 mL) was added to the water phase and this was extracted once more with EtOAc (x3). The combined organic phases was dried over MgSO<sub>4</sub> and concentrated *in vacuo* to give 103 mg (76%) of a white solid: *t*<sub>R</sub> = 8.74 min (94.5%); <sup>1</sup>H NMR (400 MHz, DMSO)  $\delta$  12.10 (br s, 1H), 8.30 (br s, 2H), 7.41–7.30 (m, 4H), 7.16–7.10 (m, 2H), 7.06–7.01 (m, 1H), 4.22–4.14 (m, 2H), 3.84–3.77 (m, 2H), 3.72 (t, *J* = 5.3 Hz, 2H), 2.96 (t, *J* = 5.3 Hz, 2H), 2.87 (t, *J* = 7.4 Hz, 2H), 2.56 (t, *J* = 7.5 Hz, 2H); <sup>13</sup>C NMR (101 MHz, DMSO)  $\delta$  173.3, 160.1 (d, *J* = 244.7 Hz), 158.3, 131.0 (d, *J* = 5.6 Hz), 130.0, 128.8 (d, *J* = 15.9 Hz), 127.6 (d, *J* = 3.1 Hz), 123.9, 123.0, 121.8 (d, *J* = 9.9 Hz), 117.7 (d, *J* = 23.9 Hz), 116.7, 116.1, 89.7, 87.9 (d, *J* = 3.1 Hz), 68.7, 67.2, 66.7, 38.3, 33.5, 23.6 (d, *J* = 2.1 Hz); ESI-HRMS calcd for C<sub>21</sub>H<sub>23</sub>FNO<sub>4</sub> (M+H<sup>+</sup>) 372.1606, found 372.1593.

*Step 2:* A dry microwave vial under argon atmosphere was charged with the deprotected crude compound from *Step 1* (14 mg, 0.04 mmol), MeOH (1 mL), NaHCO<sub>3</sub> (14 mg, 0.16 mmol) and 4-chloro-7-nitrobenzo[c][1,2,5]oxadiazole (NBD-Cl, 23 mg, 0.12 mmol). The reaction was covered with aluminum foil and stirred at 50°C for 4 hours. Afterwards the reaction was concentrated under a stream of nitrogen. The residue was dissolved in a mixture of EtOAc and 1M HCl<sub>aq</sub>. The organic phase was washed with water, brine, dried over Na<sub>2</sub>SO<sub>4</sub> and concentrated *in vacuo*. The crude was dissolved in minimum amount of MeCN and MeOH and purified by preparative HPLC with fraction collection at 365 nm using MeCN and milliQ water both containing 0.1% formic acid as modifier. The compound fraction was pooled, concentrated *in*

*vacuo* and extracted with EtOAc (x2). The organic phases were combined, washed with brine, dried over Na<sub>2</sub>SO<sub>4</sub> and concentrated *in vacuo* to give 11 mg (54%) of **2** as an orange solid (*t*<sub>R</sub> = 12.33 min, purity >99% by HPLC). All handling was performed in dimmed lightning and solutions were stored in aluminum foil-covered glassware. <sup>1</sup>H NMR (400 MHz, DMSO-*d*<sub>6</sub>) δ 8.32 (d, *J* = 7.5 Hz, 1H), 7.48–7.28 (m, 6H), 7.20–7.07 (m, 3H), 7.00 (d, *J* = 7.5 Hz, 1H), 6.37 (d, *J* = 8.5 Hz, 1H), 4.24–4.15 (m, 3H), 3.93–3.81 (m, 5H), 3.79–3.66 (m, 2H), 2.89 (t, *J* = 7.2 Hz, 3H), 2.50 (t, *J* = 7.5 Hz, 3H); ESI-HRMS calcd for C<sub>27</sub>H<sub>23</sub>FN<sub>4</sub>NaO<sub>7</sub> (M+Na)<sup>+</sup> 557.1443, found 557.1416.

**3-(2-Fluoro-4-((2'-methyl-4'-(2-(2-((7-nitrobenzo[*c*][1,2,5]oxadiazol-4-yl)amino)ethoxy)ethoxy)-[1,1'-biphenyl]-3-yl)methoxy)phenyl)propanoic acid.** (4) *Step 1:* Boc-protected amine **11** (83 mg, 0.14 mmol) was dissolved in THF (1.7 mL) and 4M HCl<sub>aq</sub> (0.8 mL) was added. The reaction was refluxed for 7 hours and after completion cooled to room temperature. 2M NaOH<sub>aq</sub> (3 mL) was added and the mixture was extracted with EtOAc/MeOH (9:1, x3). The organic phases were collected, dried over Na<sub>2</sub>SO<sub>4</sub> and concentrated *in vacuo* giving the zwitterion as a beige solid that was used directly in the next step.

*Step 2:* A dry flask under argon with magnetic stirring bar was charged with the crude material from *Step 1* (0.14 mmol), MeOH (3.7 mL), NaHCO<sub>3</sub> (37 mg, 0.45 mmol) and 4-chloro-7-nitrobenzo[*c*][1,2,5]oxadiazole (NBD-Cl, 86 mg, 0.43 mmol). The reaction was covered with aluminum foil and heated to 50°C for 4¼ hours. The reaction was concentrated under a gentle flow of nitrogen and the crude was dissolved in 1 M HCl<sub>aq</sub> and EtOAc. The mixture was extracted and phases separated, and the water phase was extracted once more with EtOAc. The organic phases were combined, washed with brine and dried over Na<sub>2</sub>SO<sub>4</sub>. The residue was concentrated and stored in the freezer overnight. The crude was dissolved in MeCN (1.5 mL) and

MeOH (0.5 mL) and purified by preparative HPLC with fraction collection at 365 nm using MeCN and milliQ water both containing 0.1% formic acid as modifier. The compound fraction was pooled, concentrated *in vacuo* and extracted with EtOAc (x2). The organic phases were combined, washed with brine, dried over Na<sub>2</sub>SO<sub>4</sub> and concentrated *in vacuo* to give 24 mg (28% over 2 steps) of **4** as an orange solid ( $t_R = 12.98$  min, purity >98.6% by HPLC). All handling was performed in dimmed lightning and solutions were stored in aluminum foil-covered glassware. <sup>1</sup>H NMR (400 MHz, DMSO)  $\delta$  12.14 (s, 1H), 9.49 (br s, 1H), 8.48 (d,  $J = 9.1$  Hz, 1H), 7.46–7.36 (m, 2H), 7.35–7.31 (m, 1H), 7.26–7.17 (m, 2H), 7.06–7.01 (m, 1H), 6.90–6.78 (m, 2H), 6.76–6.71 (m, 2H), 6.49 (d,  $J = 9.0$  Hz, 1H), 5.13 (s, 2H), 4.10–4.06 (m, 2H), 3.80 (dd,  $J = 10.1, 5.2$  Hz, 4H), 3.70 (br s, 2H), 2.76 (t,  $J = 7.5$  Hz, 2H), 2.48–2.43 (m, 2H), 2.13 (s, 3H); ESI-HRMS calcd for C<sub>31</sub>H<sub>31</sub>FN<sub>4</sub>NaO<sub>8</sub> (M+Na)<sup>+</sup> 653.2018, found 653.1995.

**Methyl 3-(4-((3-(2-(2-((*tert*-butoxycarbonyl)amino)ethoxy)ethoxy)phenyl)ethynyl)-2-fluorophenyl)propanoate (7).** 2-(2-(*N*-Boc-amino)ethoxy)ethyl tosylate (276 mg, 0.77 mmol), **6** (149 mg, 0.50 mmol), MeCN (2 mL) and K<sub>2</sub>CO<sub>3</sub> (147 mg, 1.06 mmol) was added to a dry flask under argon. The reaction was refluxed for 3½ h, cooled to room temperature and diluted with water before extraction with EtOAc (x3). The combined organic phases were washed with brine, dried over MgSO<sub>4</sub> and concentrated *in vacuo*. The residue was purified by flash chromatography (SiO<sub>2</sub>, EtOAc:petroleum ether, 1:3) to give 192 mg (79%) of a white solid:  $R_f = 0.40$  (EtOAc:petroleum ether, 1:1); <sup>1</sup>H NMR (400 MHz, CDCl<sub>3</sub>)  $\delta$  7.29–7.15 (m, 4H), 7.14–7.10 (m, 1H), 7.09–7.05 (m, 1H), 6.93 (dd,  $J = 8.3, 1.8$  Hz, 1H), 4.97 (br s, 1H), 4.18–4.09 (m, 2H), 3.87–3.79 (m, 2H), 3.68 (s, 3H), 3.62 (t,  $J = 5.1$  Hz, 2H), 3.40–3.29 (m, 2H), 2.99 (t,  $J = 7.7$  Hz, 2H), 2.64 (t,  $J = 7.7$  Hz, 2H), 1.45 (s, 9H); <sup>13</sup>C NMR (101 MHz, CDCl<sub>3</sub>)  $\delta$  172.9, 160.6 (d,  $J = 246.3$  Hz), 158.5, 130.6 (d,  $J = 5.6$  Hz), 129.5, 128.1 (d,  $J = 16.0$  Hz), 127.5 (d,  $J = 3.2$  Hz), 124.5,

123.9, 123.1 (d,  $J = 9.8$  Hz), 118.3 (d,  $J = 23.8$  Hz), 117.2, 115.8, 89.8, 88.0 (d,  $J = 3.3$  Hz), 79.3, 70.5, 69.4, 67.4, 51.7, 40.4, 34.0, 28.4, 24.6 (d,  $J = 2.3$  Hz).

**Ethyl 3-(4-((3-bromobenzyl)oxy)-2-fluorophenyl)propanoate (9).** A flask was charged with 3-bromobenzyl bromide (256 mg, 1.03 mmol), **8** (203 mg, 0.96 mmol),  $K_2CO_3$  (281 mg, 2.03 mmol) and acetone (5 mL), and the reaction mixture was stirred at room temperature for 16 hours. After completion, as indicated by TLC, the reaction was diluted with water and extracted with EtOAc (x3). The organic phases were combined, washed with brine, dried over  $Na_2SO_4$  and concentrated *in vacuo*. The residue was purified by flash chromatography ( $SiO_2$ , EtOAc:petroleum ether, 1:6) to give 297 mg (81%) of **9** as a clear oil:  $R_f = 0.39$  (EtOAc:petroleum ether, 1:4);  $^1H$  NMR (400 MHz,  $CDCl_3$ )  $\delta$  7.59–7.55 (m, 1H), 7.49–7.44 (m, 1H), 7.35–7.31 (m, 1H), 7.28–7.23 (m, 1H), 7.14–7.08 (m, 1H), 6.70–6.61 (m, 2H), 4.99 (s, 2H), 4.12 (q,  $J = 7.1$  Hz, 2H), 2.91 (t,  $J = 7.7$  Hz, 2H), 2.59 (t,  $J = 7.7$  Hz, 2H), 1.23 (t,  $J = 7.1$  Hz, 3H);  $^{13}C$  NMR (101 MHz,  $CDCl_3$ )  $\delta$  172.9, 161.6 (d,  $J = 245.6$  Hz), 158.4 (d,  $J = 10.9$  Hz), 139.1, 131.3, 131.1 (d,  $J = 6.8$  Hz), 130.5, 130.3, 126.0, 122.9, 120.0 (d,  $J = 16.2$  Hz), 110.6 (d,  $J = 3.1$  Hz), 102.8 (d,  $J = 25.7$  Hz), 69.5, 60.6, 34.8 (d,  $J = 1.2$  Hz), 24.2 (d,  $J = 2.1$  Hz), 14.4; ESI-HRMS calcd for  $C_{18}H_{18}BrFNaO_3$  ( $M+Na$ ) $^+$  403.0316, found 403.0300.

**Ethyl 3-(2-fluoro-4-((4'-hydroxy-2'-methyl-[1,1'-biphenyl]-3-yl)methoxy)phenyl)propanoate (10).** A Schlenk flask with magnetic stirring bar under  $N_2$  flow was charged with tetrahydroxydiboron (BBA, 135 mg, 1.51 mmol), KOAc (152 mg, 1.54 mmol), Xphos (5 mg, 2mol%), Xphos-Pd-G2 (4 mg, 1mol%) and **9** (180 mg, 0.47 mmol) dissolved in EtOH (5 mL). The mixture was evacuated and backfilled with argon (x3) and heated to 80°C. After 1½ hour the reaction had turned orange and 1.8M  $K_2CO_{3aq}$  (0.9 mL) and 4-bromo-3-methylphenol (121 mg, 0.65 mmol) dissolved in EtOH (0.5 mL) was added. The mixture was evacuated and backfilled

with argon (x3) once again and at stirred at 80°C overnight. The reaction was cooled to room temperature, diluted with water and extracted with EtOAc (x3). The organic phases were combined, washed with brine, dried over Na<sub>2</sub>SO<sub>4</sub> and concentrated *in vacuo*. The residue was purified by flash chromatography (SiO<sub>2</sub>, EtOAc:petroleum ether, 1:4) to give 71mg (37%) of **10** as a red sticky oil:  $R_f = 0.14$  (EtOAc:petroleum ether, 1:4); <sup>1</sup>H NMR (400 MHz, CDCl<sub>3</sub>)  $\delta$  7.44–7.32 (m, 3H), 7.28–7.24 (m, 1H), 7.13–7.07 (m, 2H), 6.77–6.65 (m, 4H), 5.06 (s, 2H), 4.87 (s, 1H), 4.12 (q,  $J = 7.1$  Hz, 2H), 2.91 (t,  $J = 7.7$  Hz, 2H), 2.59 (t,  $J = 7.7$  Hz, 2H), 2.21 (s, 3H), 1.23 (t,  $J = 7.1$  Hz, 3H); <sup>13</sup>C NMR (101 MHz, CDCl<sub>3</sub>)  $\delta$  173.0, 161.6 (d,  $J = 245.3$  Hz), 158.7 (d,  $J = 10.9$  Hz), 155.0, 142.1, 137.2, 136.5, 134.5, 131.2, 131.0 (d,  $J = 6.8$  Hz), 129.3, 128.7, 128.5, 125.8, 119.7 (d,  $J = 16.2$  Hz), 117.1, 112.9, 110.7, 102.8 (d,  $J = 25.7$  Hz), 70.5, 60.6, 34.9 (d,  $J = 1.1$  Hz), 24.2 (d,  $J = 1.9$  Hz), 20.7, 14.3; ESI-HRMS calcd for C<sub>25</sub>H<sub>25</sub>FNaO<sub>4</sub> (M+Na)<sup>+</sup> 431.1629, found 431.1610.

**Ethyl 3-(4-((4'-(2-(2-((tert-butoxycarbonyl)amino)ethoxy)ethoxy)-2'-methyl-[1,1'-biphenyl]-3-yl)methoxy)-2-fluorophenyl)propanoate (11).** A flask under argon was charged with **7** (64 mg, 0.16 mmol), K<sub>2</sub>CO<sub>3</sub> (62 mg, 0.45 mmol) and 2-(2-(*N*-Boc-amino)ethoxy)ethyl tosylate (123 mg, 0.34 mmol) dissolved in MeCN (4 mL), and the mixture was refluxed for 23 hours. The reaction was cooled to room temperature, diluted with water and extracted with EtOAc (x3). The organic phases were combined, washed with brine, dried over Na<sub>2</sub>SO<sub>4</sub> and concentrated *in vacuo*. The residue was purified by flash chromatography (SiO<sub>2</sub>, EtOAc:petroleum ether, 1:2) to give 87 mg (93%) of **11** as a clear sticky oil:  $R_f = 0.15$  (EtOAc:petroleum ether, 1:3); <sup>1</sup>H NMR (400 MHz, CDCl<sub>3</sub>)  $\delta$  7.44–7.32 (m, 3H), 7.29–7.24 (m, 1H), 7.17–7.07 (m, 2H), 6.86–6.79 (m, 2H), 6.72–6.65 (m, 2H), 5.06 (s, 2H), 4.18–4.07 (m, 4H), 3.86–3.80 (m, 2H), 3.63 (t,  $J = 5.2$  Hz, 2H), 3.36 (d,  $J = 5.2$  Hz, 2H), 2.90 (t,  $J = 7.7$  Hz, 2H),

2.58 (t,  $J = 7.7$  Hz, 2H), 2.23 (s, 3H), 1.45 (s, 9H), 1.23 (t,  $J = 7.1$  Hz, 3H); ESI-MS  $m/z$  618.3 (M+Na<sup>+</sup>).

### **Characterization of excitation and emission properties of fluorescent ligands for FFA1**

Absorbance curves and extinction coefficients for fluorescent ligands dissolved in either *n*-octanol or HBSS (with Ca<sup>2+</sup> and Mg<sup>2+</sup>) were measured in triplicate using a FLUOstar Omega Microplate Reader (BMG LAB-TECH).

Emission curves for fluorescent ligands were measured in duplicate using a ChronosFD time-resolved spectrofluorometer coupled to PMT detectors. All compounds were excited at a fixed excitation wavelength of 402 nm, and coumarin 153 (C-153) in EtOH was used as an internal standard for determination of quantum yield ( $\phi_{C-153} = 0.546$ ,  $\lambda_{ex} = 402$  nm)<sup>29</sup>. All experiments were performed at 25°C.

### **Ca<sup>2+</sup> mobilization**

Ca<sup>2+</sup> mobilization experiments were conducted using either Flp-In T-REx 293 cells engineered to express FFA1-eYFP in an inducible fashion in response to the antibiotic doxycycline, or in N1-FFA1 cells that constitutively expressed untagged FFA1. Cells were plated (50,000/well for Flp-In T-REx 293 cells or 15,000/well for N1-FFA1 cells) in black with clear bottom 96 well cell culture plates 24 h prior to experiments. At the time of plating the Flp-In T-REx 293 cells were also treated with 100 ng/ml doxycycline to induce FFA1-eYFP expression. Prior to the assay cells were loaded for 45 min with the Ca<sup>2+</sup> dye, Fura-2 AM. Cells were then washed three times and incubated for 15 minutes in HBSS. Fura-2 fluorescent emission at 510 nm resulting from 340 or 380 nm excitation was then monitored using a Flexstation plate reader (Molecular Devices, Sunnyvale, CA, USA), both before and for 90 s after the addition of test compounds.

The peak 340/380 ratio obtained after compound addition was then used to plot concentration-response data and determine compound potency.

### **β Arrestin-2 BRET**

Plasmids encoding human FFA1 fused at its C-terminal to enhanced yellow fluorescent protein was co-transfected into HEK 293 cells with a plasmid encoding  $\beta$ -arrestin-2 fused to Renilla luciferase. Cells were distributed into white 96-well plates 24 h post-transfection and then maintained in culture for another 24 h prior to their use. To conduct the assay, cells were first washed in HBSS and then the Renilla luciferase substrate coelenterazine h (2.5  $\mu$ M) and the ligand of interest were added. Cells were incubated at 37 °C for 5 min before luminescence at 535 and 475 nm was measured using a Pherastar FS plate reader. The ratio of luminescence at 535/475 nm was then used to calculate the BRET response.

### **Development of NLUC-FFA1 construct and cell line**

In order to develop a BRET binding assay a DNA construct was first generated using a seamless DNA assembly kit (Life Technologies) encoding the NLUC sequence immediately upstream and in-frame with the FFA1 coding sequence. To ensure proper cell surface delivery, the signal peptide sequence of the mGluR5 glutamate receptor was also included immediately upstream of the NLUC coding sequence. This construct was then transfected into Flp-In T-REx 293 cells to generate a stable inducible cell line that expresses NLUC-FFA1 in response to doxycycline. The functionality of this construct and cell line to responded to FFA1 agonists was demonstrated through  $\text{Ca}^{2+}$  assays.

### **Equilibrium BRET binding assay**

NLUC-FFA1 Flp-In T-REx 293 cells were induced to express the receptor construct by treatment for 24 h with 100 ng/ml doxycycline. Cells were then harvested and used to make total

cell membrane preparations according to a previously described protocol.<sup>30</sup> Membranes were then resuspended in assay buffer (50 mM HEPES, 100 mM NaCl, 10 mM CaCl<sub>2</sub>, 10 mM MgCl<sub>2</sub>) and distributed into the wells of a white 96 well plate (5µg membrane protein/well). Membranes were then co-incubated with the indicated concentration of **4** (and **5** for non-specific binding measurements; or competing ligand for competition experiments) for 1 h at 25 °C. Following incubation, the NLUC substrate, Nano-Glo (Promega) was added to a final 1:800 dilution. Membranes were incubated a further 5 minutes before the bioluminescent emission at 460nm and 545 nm was measured using a Clariostar plate reader (BMG labtech). The ratio of 545/460 was then background subtracted and multiplied by 1000 to yield 'Net mBRET' units. Total and non-specific saturation binding data were then globally fit to a one-site binding model using Graphpad Prism v6. Competition binding experiments were fit to a one-site model, and used to calculate  $pK_i$  values based on a  $K_d$  value for **4** of 7.4 nM.

#### **Kinetic BRET binding assay**

For kinetic BRET binding assays, cell membranes were generated as for the equilibrium binding assay and again distributed in white 96 well microplates (2.5 µg membrane protein/well). The Nano-Glo substrate was then added (1:800 final dilution) before incubation for 5 min at 25 °C. Plates were then inserted into a Clariostar plate reader, with temperature set to 25 °C and set to read bioluminescent emission at 460 nm and 545 nm at 20 s intervals. After 60 s, association experiments were initiated by the injection of **4** (100 nM final concentration) into the reaction using the Clariostar injectors. Readings were continued at 20 s intervals. 5 min after **4** had been added dissociation experiments were initiated by the injection of **5** (to a 10 µM final concentration), and readings were taken for a further 15 min. In all kinetic experiments parallel wells were run where **5** had been pre-added and these were used to subtract the non-

specific binding signal for **4**. Kinetic binding data were then fit to a combined association then dissociation model using Graphpad Prism v6 in order to obtain estimates of  $K_{\text{off}}$ ,  $K_{\text{on}}$  and  $K_{\text{d}}$ .

#### ASSOCIATED CONTENT

**Supporting Information.** Absorption and emission spectra of **2**. Competition binding curves for **1**, **3**, **5**, **12** and lauric acid. This material is available free of charge via the Internet at <http://pubs.acs.org>.

#### AUTHOR INFORMATION

##### **Corresponding Author**

\*Tel: +45 6550 2568. E-mail: [ulven@sdu.dk](mailto:ulven@sdu.dk)

##### **Author Contributions**

The manuscript was written through contributions of all authors. All authors have given approval to the final version of the manuscript.

##### **Funding Sources**

The study has been funded by the Danish Council for Independent Research | Technology and Production Sciences (grant 09-070364), the Danish Council for Strategic Research (grant 11-116196) and the University of Southern Denmark. EC is supported by a fellowship from the Lundbeck Foundation. BDH is supported by a fellowship from the University of Glasgow.

##### **Notes**

BDH, GM and TU are shareholders of Caldan Therapeutics.

#### ACKNOWLEDGMENT

We thank Lone Overgaard Storm for excellent technical assistance.

## ABBREVIATIONS

7TM, seven transmembrane; BODIPY, 4,4-difluoro-4-bora-3a,4a-diaza-s-indacene; BRET, bioluminescence resonance energy transfer; DHA, docosahexaenoic acid; FFA1, free fatty acid receptor 1; HBSS, Hanks' balanced salt solution; NBD, 4-nitro-7-aminobenzodiazole; NLUC, NanoLuciferase; SS, Stokes shift; RLU, relative luminescence units; XPhos, 2-dicyclohexylphosphino-2',4',6'-triisopropylbiphenyl.

## REFERENCES

1. (a) Briscoe, C. P.; Tadayyon, M.; Andrews, J. L.; Benson, W. G.; Chambers, J. K.; Eilert, M. M.; Ellis, C.; Elshourbagy, N. A.; Goetz, A. S.; Minnick, D. T.; Murdock, P. R.; Sauls, H. R., Jr.; Shabon, U.; Spinage, L. D.; Strum, J. C.; Szekeres, P. G.; Tan, K. B.; Way, J. M.; Ignar, D. M.; Wilson, S.; Muir, A. I., The orphan G protein-coupled receptor GPR40 is activated by medium and long chain fatty acids. *The Journal of biological chemistry* **2003**, *278* (13), 11303-11; (b) Itoh, Y.; Kawamata, Y.; Harada, M.; Kobayashi, M.; Fujii, R.; Fukusumi, S.; Ogi, K.; Hosoya, M.; Tanaka, Y.; Uejima, H.; Tanaka, H.; Maruyama, M.; Satoh, R.; Okubo, S.; Kizawa, H.; Komatsu, H.; Matsumura, F.; Noguchi, Y.; Shinohara, T.; Hinuma, S.; Fujisawa, Y.; Fujino, M., Free fatty acids regulate insulin secretion from pancreatic beta cells through GPR40. *Nature* **2003**, *422* (6928), 173-6; (c) Kotarsky, K.; Nilsson, N. E.; Flodgren, E.; Owman, C.; Olde, B., A human cell surface receptor activated by free fatty acids and thiazolidinedione drugs. *Biochemical and biophysical research communications* **2003**, *301* (2), 406-10.
2. (a) Edfalk, S.; Steneberg, P.; Edlund, H., Gpr40 is expressed in enteroendocrine cells and mediates free fatty acid stimulation of incretin secretion. *Diabetes* **2008**, *57* (9), 2280-2287; (b) Liou, A. P.; Lu, X.; Sei, Y.; Zhao, X.; Pechhold, S.; Carrero, R. J.; Raybould, H. E.; Wank, S., The G-protein-coupled receptor GPR40 directly mediates long-chain fatty acid-induced secretion of cholecystokinin. *Gastroenterology* **2011**, *140* (3), 903-12; (c) Hauge, M.; Vestmar, M. A.; Husted, A. S.; Ekberg, J. P.; Wright, M. J.; Di Salvo, J.; Weinglass, A. B.; Engelstoft, M. S.; Madsen, A. N.; Lückmann, M.; Miller, M. W.; Trujillo, M. E.; Frimurer, T. M.; Holst, B.; Howard, A. D.; Schwartz, T. W., GPR40 (FFAR1) – Combined Gs and Gq signaling in vitro is associated with robust incretin secretagogue action ex vivo and in vivo. *Molecular metabolism* **2015**, *4* (1), 3-14.
3. Burant, C. F.; Viswanathan, P.; Marcinak, J.; Cao, C.; Vakilynejad, M.; Xie, B.; Leifke, E., TAK-875 versus placebo or glimepiride in type 2 diabetes mellitus: a phase 2, randomised, double-blind, placebo-controlled trial. *Lancet* **2012**, *379* (9824), 1403-11.
4. (a) Sasaki, S.; Kitamura, S.; Negoro, N.; Suzuki, M.; Tsujihata, Y.; Suzuki, N.; Santou, T.; Kanzaki, N.; Harada, M.; Tanaka, Y.; Kobayashi, M.; Tada, N.; Funami, M.; Tanaka, T.; Yamamoto, Y.; Fukatsu, K.; Yasuma, T.; Momose, Y., Design, synthesis, and biological activity of potent and orally available G protein-coupled receptor 40 agonists. *Journal of medicinal chemistry* **2011**, *54* (5), 1365-78; (b) Negoro, N.; Sasaki, S.; Mikami, S.; Ito, M.; Tsujihata, Y.; Ito, R.; Suzuki, M.; Takeuchi, K.; Suzuki, N.; Miyazaki, J.; Santou, T.; Odani, T.; Kanzaki, N.; Funami, M.; Morohashi, A.; Nonaka, M.; Matsunaga, S.; Yasuma, T.; Momose, Y., Optimization

- of (2,3-dihydro-1-benzofuran-3-yl)acetic acids: discovery of a non-free fatty acid-like, highly bioavailable G protein-coupled receptor 40/free fatty acid receptor 1 agonist as a glucose-dependent insulinotropic agent. *Journal of medicinal chemistry* **2012**, *55* (8), 3960-74.
5. Yabuki, C.; Komatsu, H.; Tsujihata, Y.; Maeda, R.; Ito, R.; Matsuda-Nagasumi, K.; Sakuma, K.; Miyawaki, K.; Kikuchi, N.; Takeuchi, K.; Habata, Y.; Mori, M., A novel antidiabetic drug, fasiglifam/TAK-875, acts as an ago-allosteric modulator of FFAR1. *PLoS One* **2013**, *8* (10), e76280.
  6. Lin, D. C. H.; Guo, Q.; Luo, J.; Zhang, J.; Nguyen, K.; Chen, M.; Tran, T.; Dransfield, P. J.; Brown, S. P.; Houze, J.; Vimolratana, M.; Jiao, X. Y.; Wang, Y.; Birdsall, N. J. M.; Swaminath, G., Identification and Pharmacological Characterization of Multiple Allosteric Binding Sites on the Free Fatty Acid 1 Receptor. *Molecular pharmacology* **2012**, *82* (5), 843-59.
  7. Srivastava, A.; Yano, J.; Hirozane, Y.; Kefala, G.; Gruswitz, F.; Snell, G.; Lane, W.; Ivetac, A.; Aertgeerts, K.; Nguyen, J.; Jennings, A.; Okada, K., High-resolution structure of the human GPR40 receptor bound to allosteric agonist TAK-875. *Nature* **2014**, *513* (7516), 124-7.
  8. Ma, Z.; Du, L.; Li, M., Toward Fluorescent Probes for G-Protein-Coupled Receptors (GPCRs). *J. Med. Chem.* **2014**, *57* (20), 8187-8203.
  9. (a) Vernall, A. J.; Hill, S. J.; Kellam, B., The evolving small-molecule fluorescent-conjugate toolbox for Class A GPCRs. *British journal of pharmacology* **2014**, *171* (5), 1073-84; (b) Sridharan, R.; Zuber, J.; Connelly, S. M.; Mathew, E.; Dumont, M. E., Fluorescent approaches for understanding interactions of ligands with G protein coupled receptors. *Biochimica et Biophysica Acta (BBA) - Biomembranes* **2014**, *1838* (1, Part A), 15-33.
  10. (a) Shi, W.; Ma, H., Spectroscopic probes with changeable pi-conjugated systems. *Chem. Commun.* **2012**, *48* (70), 8732-44; (b) Loudet, A.; Burgess, K., BODIPY dyes and their derivatives: syntheses and spectroscopic properties. *Chem. Rev.* **2007**, *107* (11), 4891-932; (c) Norager, N. G.; Jensen, C. B.; Rathje, M.; Andersen, J.; Madsen, K. L.; Kristensen, A. S.; Stromgaard, K., Development of potent fluorescent polyamine toxins and application in labeling of ionotropic glutamate receptors in hippocampal neurons. *ACS Chem. Biol.* **2013**, *8* (9), 2033-41; (d) Heisig, F.; Gollos, S.; Freudenthal, S. J.; El-Tayeb, A.; Iqbal, J.; Muller, C. E., Synthesis of BODIPY derivatives substituted with various bioconjugatable linker groups: a construction kit for fluorescent labeling of receptor ligands. *Journal of fluorescence* **2014**, *24* (1), 213-30.
  11. Uchiyama, S.; Santa, T.; Okiyama, N.; Fukushima, T.; Imai, K., Fluorogenic and fluorescent labeling reagents with a benzofurazan skeleton. *Biomedical Chromatography* **2001**, *15* (5), 295-318.
  12. Uchiyama, S.; Santa, T.; Fukushima, T.; Homma, H.; Imai, K., Effects of the substituent groups at the 4- and 7-positions on the fluorescence characteristics of benzofurazan compounds. *J. Chem. Soc., Perkin Trans. 2* **1998**, (10), 2165-2174.
  13. Toyooka, T.; Watanabe, Y.; Imai, K., Reaction of amines of biological importance with 4-fluoro-7-nitrobenzo-2-oxa-1,3-diazole. *Anal. Chim. Acta* **1983**, *149*, 305-12.
  14. Lin, S.; Struve, W. S., Time-resolved fluorescence of nitrobenzoxadiazole-aminohexanoic acid: effect of intermolecular hydrogen-bonding on non-radiative decay. *Photochem. Photobiol.* **1991**, *54* (3), 361-5.
  15. (a) Turcatti, G.; Vogel, H.; Chollet, A., Probing the binding domain of the NK2 receptor with fluorescent ligands: evidence that heptapeptide agonists and antagonists bind differently. *Biochemistry* **1995**, *34* (12), 3972-80; (b) Petrov, R. R.; Ferrini, M. E.; Jaffar, Z.; Thompson, C. M.; Roberts, K.; Diaz, P., Design and evaluation of a novel fluorescent CB2 ligand as probe for receptor visualization in immune cells. *Bioorg. Med. Chem. Lett.* **2011**, *21* (19), 5859-5862.

16. Christiansen, E.; Hansen, S. V.; Urban, C.; Hudson, B. D.; Wargent, E. T.; Grundmann, M.; Jenkins, L.; Zaibi, M.; Stocker, C. J.; Ullrich, S.; Kostenis, E.; Kassack, M. U.; Milligan, G.; Cawthorne, M. A.; Ulven, T., Discovery of TUG-770: A Highly Potent Free Fatty Acid Receptor 1 (FFA1/GPR40) Agonist for Treatment of Type 2 Diabetes. *ACS Med. Chem. Lett.* **2013**, *4* (5), 441-445.
17. Christiansen, E.; Due-Hansen, M. E.; Urban, C.; Grundmann, M.; Schmidt, J.; Hansen, S. V.; Hudson, B. D.; Zaibi, M.; Markussen, S. B.; Hagesaether, E.; Milligan, G.; Cawthorne, M. A.; Kostenis, E.; Kassack, M. U.; Ulven, T., Discovery of a potent and selective free fatty acid receptor 1 agonist with low lipophilicity and high oral bioavailability. *Journal of medicinal chemistry* **2013**, *56* (3), 982-92.
18. Christiansen, E.; Due-Hansen, M. E.; Urban, C.; Grundmann, M.; Schroder, R.; Hudson, B. D.; Milligan, G.; Cawthorne, M. A.; Kostenis, E.; Kassack, M. U.; Ulven, T., Free fatty acid receptor 1 (FFA1/GPR40) agonists: mesylpropoxy appendage lowers lipophilicity and improves ADME properties. *Journal of medicinal chemistry* **2012**, *55* (14), 6624-8.
19. Christiansen, E.; Due-Hansen, M. E.; Urban, C.; Merten, N.; Pfeleiderer, M.; Karlsen, K. K.; Rasmussen, S. S.; Steensgaard, M.; Hamacher, A.; Schmidt, J.; Drewke, C.; Petersen, R. K.; Kristiansen, K.; Ullrich, S.; Kostenis, E.; Kassack, M. U.; Ulven, T., Structure-Activity Study of Dihydrocinnamic Acids and Discovery of the Potent FFA1 (GPR40) Agonist TUG-469. *ACS Med. Chem. Lett.* **2010**, *1* (7), 345-9.
20. El-Gendy, B. E.-D. M.; Zadeh, E. H. G.; Sotuyo, A. C.; Pillai, G. G.; Katritzky, A. R.,  $\pm$ -substitution effects on the ease of S' N-acyl transfer in aminothioesters. *Chem. Biol. Drug Des.* **2013**, *81* (5), 577-582.
21. Molander, G. A.; Trice, S. L.; Kennedy, S. M., Scope of the two-step, one-pot palladium-catalyzed borylation/Suzuki cross-coupling reaction utilizing bis-boronic acid. *J. Org. Chem.* **2012**, *77* (19), 8678-88.
22. Stoddart, L. A.; Johnstone, E. K.; Wheal, A. J.; Goulding, J.; Robers, M. B.; Machleidt, T.; Wood, K. V.; Hill, S. J.; Pflieger, K. D., Application of BRET to monitor ligand binding to GPCRs. *Nat. Methods* **2015**, *12* (7), 661-3.
23. Briscoe, C. P.; Peat, A. J.; McKeown, S. C.; Corbett, D. F.; Goetz, A. S.; Littleton, T. R.; McCoy, D. C.; Kenakin, T. P.; Andrews, J. L.; Ammala, C.; Fornwald, J. A.; Ignar, D. M.; Jenkinson, S., Pharmacological regulation of insulin secretion in MIN6 cells through the fatty acid receptor GPR40: identification of agonist and antagonist small molecules. *British journal of pharmacology* **2006**, *148* (5), 619-28.
24. Houze, J. B.; Zhu, L.; Sun, Y.; Akerman, M.; Qiu, W.; Zhang, A. J.; Sharma, R.; Schmitt, M.; Wang, Y.; Liu, J.; Liu, J.; Medina, J. C.; Reagan, J. D.; Luo, J.; Tonn, G.; Zhang, J.; Lu, J. Y.; Chen, M.; Lopez, E.; Nguyen, K.; Yang, L.; Tang, L.; Tian, H.; Shuttleworth, S. J.; Lin, D. C., AMG 837: a potent, orally bioavailable GPR40 agonist. *Bioorganic & medicinal chemistry letters* **2012**, *22* (2), 1267-70.
25. Tan, C. P.; Feng, Y.; Zhou, Y. P.; Eiermann, G. J.; Petrov, A.; Zhou, C.; Lin, S.; Salituro, G.; Meinke, P.; Mosley, R.; Akiyama, T. E.; Einstein, M.; Kumar, S.; Berger, J. P.; Mills, S. G.; Thornberry, N. A.; Yang, L.; Howard, A. D., Selective small-molecule agonists of G protein-coupled receptor 40 promote glucose-dependent insulin secretion and reduce blood glucose in mice. *Diabetes* **2008**, *57* (8), 2211-9.
26. Negoro, N.; Sasaki, S.; Mikami, S.; Ito, M.; Suzuki, M.; Tsujihata, Y.; Ito, R.; Harada, A.; Takeuchi, K.; Suzuki, N.; Miyazaki, J.; Santou, T.; Odani, T.; Kanzaki, N.; Funami, M.; Tanaka, T.; Kogame, A.; Matsunaga, S.; Yasuma, T.; Momose, Y., Discovery of TAK-875: A

Potent, Selective, and Orally Bioavailable GPR40 Agonist. *ACS Med. Chem. Lett.* **2010**, *1* (6), 290-4.

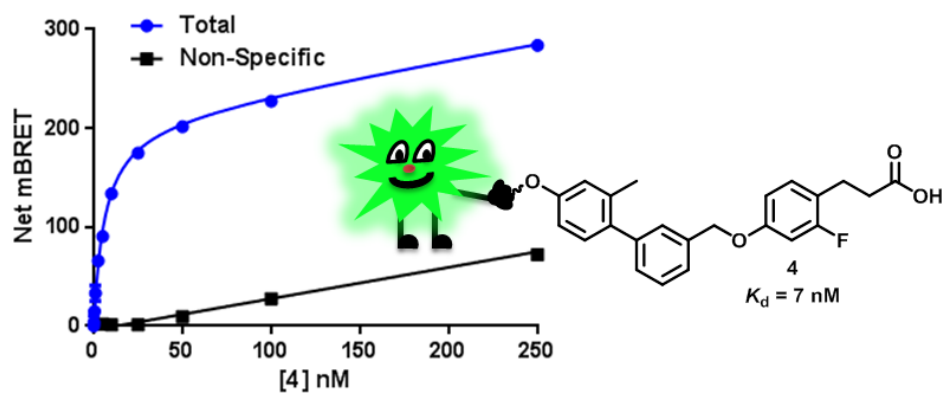
27. Christiansen, E.; Urban, C.; Merten, N.; Liebscher, K.; Karlsen, K. K.; Hamacher, A.; Spinrath, A.; Bond, A. D.; Drewke, C.; Ullrich, S.; Kassack, M. U.; Kostenis, E.; Ulven, T., Discovery of potent and selective agonists for the free fatty acid receptor 1 (FFA(1)/GPR40), a potential target for the treatment of type II diabetes. *Journal of medicinal chemistry* **2008**, *51* (22), 7061-4.

28. Charlton, S. J.; Vauquelin, G., Elusive equilibrium: the challenge of interpreting receptor pharmacology using calcium assays. *British journal of pharmacology* **2010**, *161* (6), 1250-65.

29. Rurack, K.; Spieles, M., Fluorescence Quantum Yields of a Series of Red and Near-Infrared Dyes Emitting at 600–1000 nm. *Analytical Chemistry* **2011**, *83* (4), 1232-1242.

30. Stoddart, L. A.; Smith, N. J.; Jenkins, L.; Brown, A. J.; Milligan, G., Conserved polar residues in transmembrane domains V, VI, and VII of free fatty acid receptor 2 and free fatty acid receptor 3 are required for the binding and function of short chain fatty acids. *The Journal of biological chemistry* **2008**, *283* (47), 32913-24.

## Table of Contents Graphic



## Supporting Information

# Development and characterization of a potent free fatty acid receptor 1 (FFA1) fluorescent tracer

*Elisabeth Christiansen<sup>†,1</sup>, Brian D. Hudson<sup>‡</sup>, Anders Højgaard Hansen<sup>†</sup>, Graeme Milligan<sup>‡</sup> and Trond Ulven<sup>†,\*</sup>*

*<sup>†</sup>Department of Physics, Chemistry and Pharmacy, University of Southern Denmark, Campusvej 55, DK-5230 Odense M, Denmark <sup>‡</sup>Molecular Pharmacology Group, Institute of Molecular, Cell and Systems Biology, College of Medical, Veterinary and Life Sciences, University of Glasgow, Glasgow G12 8QQ, Scotland, United Kingdom*

### Contents

Absorption & emission spectra of <b>2</b>	S2
Competition binding curves for synthetic agonists and lauric acid	S3

## Absorption & emission spectra of **2**

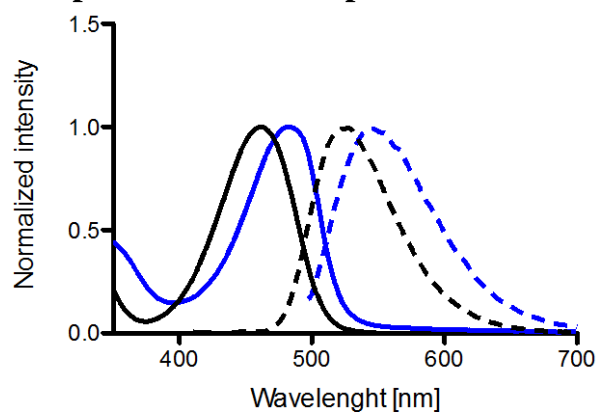


**Figure S1.** Normalized absorption and emission spectra of **2**. -- *n*-octanol, -- Hank's buffer, solid line ~ excitation, dotted line ~ emission.

## Competition binding curves for synthetic agonists and lauric acid

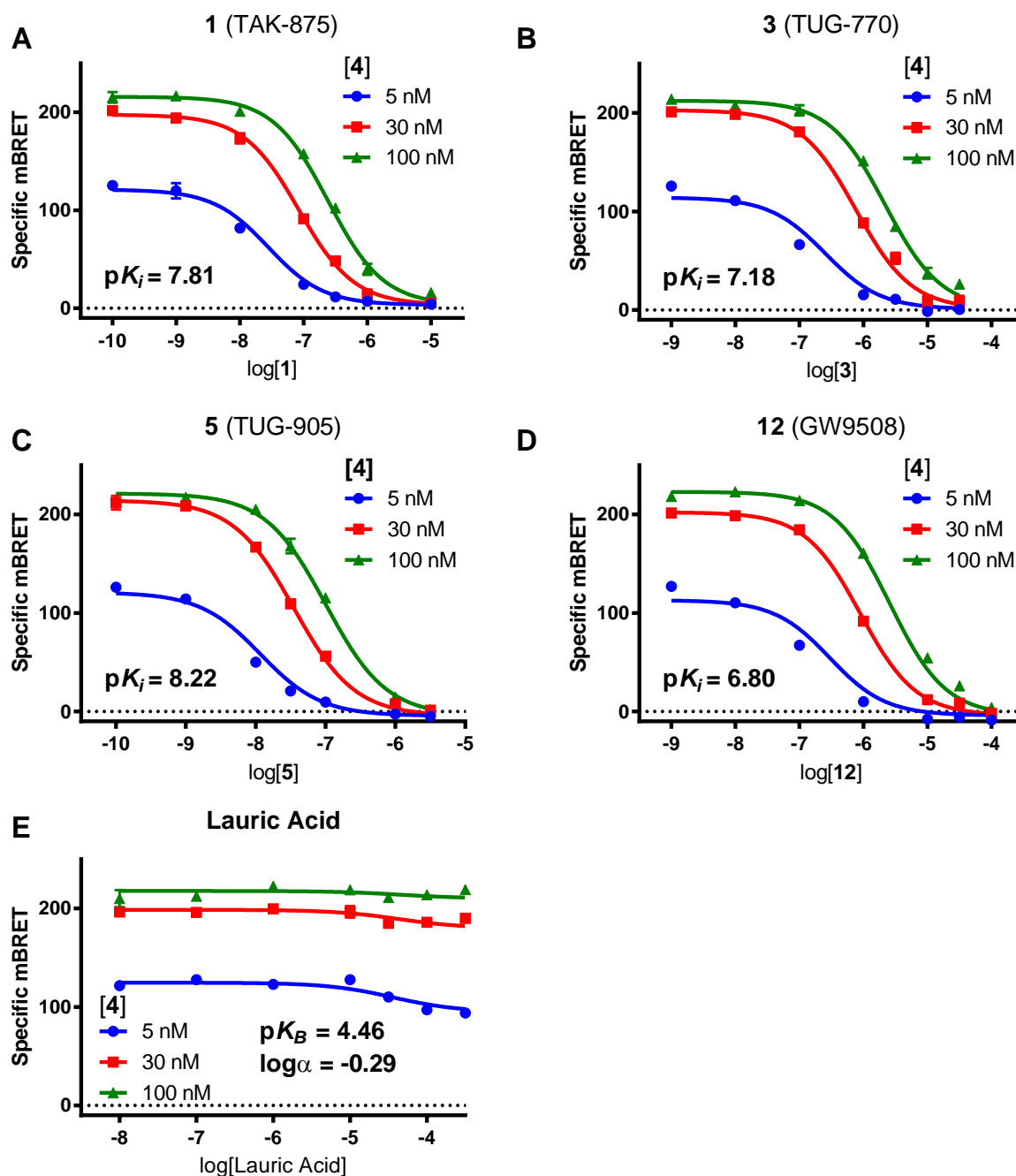


**Figure S2.** The synthetic agonists **1** (TAK-875), **3** (TUG-770), **5** (TUG-905) and **12** (GW9508), but not the saturated fatty acid, lauric acid, bind competitively to FFA1 with **4**. Competition BRET binding curves were generated using 5, 30 and 100 nM concentrations of **4** against **1** (A), **3** (B), **5** (C), **12** (D), and lauric acid (E). Each of the synthetic ligands in A-D fully displaced **4** at all three concentrations, and therefore data were fit to determine  $pK_i$ . Lauric acid did not fully compete with **4**, and therefore was fit to an allosteric ternary complex model to determine  $pK_B$  and  $\log\alpha$ . Data shown are representative of triplicate experiments.